Climatic Role of North American Low-Level Jets on U.S. Regional Tornado Activity

SCOTT J. WEAVER, STEPHEN BAXTER, AND ARUN KUMAR

NOAA/Climate Prediction Center, Camp Springs, Maryland

(Manuscript received 3 October 2011, in final form 19 March 2012)

ABSTRACT

Variability of springtime tornadic activity over the United States is assessed through the connectivity of preferred modes of North American low-level jet (NALLJ) variability to the local thermodynamic environment and remote SST variations. The link between regional tornado activity and NALLJ variability as diagnosed from a consistent reanalysis system (i.e., NCEP–NCAR) serves as dynamical corroboration in light of the inhomogeneous tornado database. The analysis reveals a multidecadal variation in the strength of the NALLJ–tornado connection, highlighted by tornado activity in the southern Great Plains region nearly doubling its correlation with NALLJ principal component 1 (PC 1) in recent decades. Locally, this is a result of a southward shift of NALLJ variability modes during the recent period. Motivated by these epochal shifts in NALLJ activity, a comparison of the early (1950–78) and late (1979–2010) tornado and NALLJ SST linkages indicates an Atlantic decadal SST variability influence during the early epoch, with Pacific decadal variability thereafter, highlighting the remote SST influence on the shifts in geographic placement and strength of NALLJ variability. The remote SST variability linkages further reveal that the observed global-scale SST trend pattern over the last 61 years may be contributing to a shift toward weaker tornadoes during spring in the northern Great Plains region. Tornado activity over the southeast region of the United States shows no such relationship to the SST trend pattern during spring, an immunity that is unexpected if spurious trends in the tornado database were influencing the SST linkage.

1. Introduction

The need for increased understanding of regional climate variability and change has recently been elevated within the national and international climate science communities. Among the many facets of this requirement is the further refinement and characterization of the linkage between extremes of weather and climate. Indeed, the societal impacts of climate variability and change are typically communicated through the weather time scale. As such, placing extreme weather phenomena in a climate context can further our scientific understanding of the characteristics of the weather–climate linkage, and therefore, regional impacts of climate variability and change.

Recent tornado outbreaks over the United States have caused devastating societal impacts with significant loss of life and property. Fortunately, the Storm Prediction Center (SPC) provided adequate warnings several days in advance of the major tornado outbreak episodes during the spring of 2011, which undoubtedly saved lives. Nevertheless, the recent call for increased understanding, attribution, and prediction of severe weather on seasonal time scales necessitates an examination of potential climate factors that influence the seasonal variability of the tornadic environment.

There is some indication that monthly-to-seasonal climate variability modulates U.S. tornado activity, and that it is not purely a result of atmospheric internal variability (Brooks et al. 2003; Shepherd et al. 2009; Frye and Mote 2010; Tippett et al. 2012). However, El Niño–Southern Oscillation (ENSO) linkages of annual U.S. tornadic activity to traditional ENSO indices (Marzaban and Schaefer 2001) and wintertime tornado outbreaks (Cook and Schaefer 2008) were shown to be weak. The intra-American seas low-level jet has been linked to March tornado activity over the Mississippi River basin through the influence of several teleconnection patterns (Muñoz and Enfield 2009). Despite the wintertime climate linkages, attribution of springtime tornadic activity to large-scale climate variability modes anchored in remote ocean basins has not been fully explored.

Corresponding author address: Dr. Scott J. Weaver, Climate Prediction Center, NOAA/NCEP/NWS, 5200 Auth Road, Rm. 605, Camp Springs, MD 20746.
E-mail: scott.weaver@noaa.gov

DOI: 10.1175/JCLI-D-11-00568.1

To be sure, warm season U.S. climate has been linked to Atlantic and Pacific decadal variability, especially precipitation (Barlow et al. 2001; Enfield et al. 2001) and Atlantic basin hurricane activity (Bell and Chelliah 2006). There is also evidence that the Pacific decadal oscillation (PDO) may act to constructively or destructively interfere with the ENSO signal with regard to the multidecadal modulation of the interannual variability in warm season U.S. climate (Hu and Huang 2009), and that warm season regional precipitation variability and its associated dynamical mechanisms has increased in the most recent 30 years when compared to the previous 30-yr period (Wang et al. 2010; Li et al. 2011).

Given this decadal modulation and the recently observed increase in the interannual variability in the dynamical mechanisms of warm season North American precipitation in the most recent decades, it is of considerable interest to assess seasonal tornadic variability in a similar context, since over large regions these precipitation generating mechanisms are apt to be similar to those linked to severe weather and tornadoes (Galway 1979). Furthermore, the local climate mechanisms that more directly force interannual variability in regional and seasonal tornadic activity, and their relationship to the spatiotemporal structure of global sea surface temperature (SST) variability, remain to be fully elucidated, including the multidecadal epochal influence.

Many factors are necessary for supporting the dynamic and thermodynamic environment conducive to the formation of tornadoes. In general it is required that high levels of atmospheric instability are present, however, it is also vital that dynamic processes are adequate to both support the highly unstable thermodynamic environment (Brooks et al. 2003), and provide the necessary triggering mechanism for the maintenance of seasonal tornadic activity. One such feature of the springtime circulation is the North American low-level jet (NALLJ), which has long been recognized as the primary mechanism for generating and focusing extreme flood events on weather and climate time scales through moisture transport, convergence, and an enhancement of atmospheric instability, most notably over the Great Plains (Weaver et al. 2009a and references therein). We refer more broadly here to the term NALLJ since it has been observed that anomalous jetlike excursions to areas outside the Great Plains are commonplace (Weaver and Nigam 2008).

In this analysis we investigate the NALLJ impact on April, May, and June (AMJ) severe weather variability through its relationship to seasonal anomalies of tornado activity over the United States and the remote SST variations. The 61-yr record is utilized here to provide a long-term (1950–2010) assessment of these linkages,

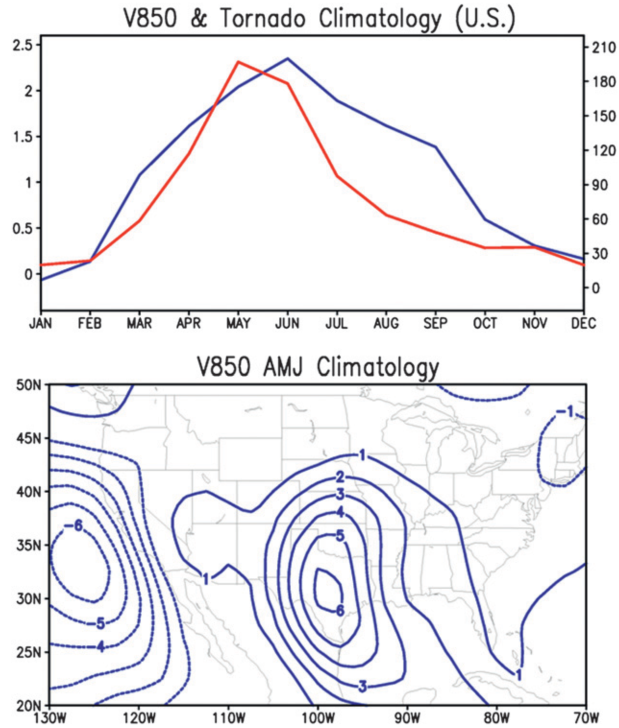

FIG. 1. (top) Monthly climatological evolution of the area averaged 20°–50°N, 105°–80°W 850-hPa meridional wind (blue) and detrended U.S. tornado counts (red) for 1950–2010. The 850-hPa meridional wind is in meters per second and the tornadoes are in raw integer counts. (bottom) Seasonal mean (AMJ) climatology of 850-hPa meridional wind from the NCEP–NCAR reanalysis for 1950–2010. 850-hPa meridional wind is contoured at 1 m s^{-1} intervals.

and to compare and contrast the interannual variability over the 1950–78 and 1979–2010 periods given the mounting evidence regarding the intensification of interannual variability of warm season precipitation in the recent decades. Investigating linkages between seasonal tornadic activity and NALLJ's from a consistent reanalysis system also provides a measure of dynamic corroboration in light of a potentially inhomogeneous tornado database.

In addition to the AMJ spring months being at the heart of the North American tornado season, the motivation is further clarified in Fig. 1, which shows the 1950–2010 U.S. monthly climatological tornado counts (red) from the SPC severe weather database (Schaefer and Edwards 1999), and 850-hPa meridional wind (blue) averaged over the eastern two-thirds of the United States (upper) and the mean AMJ low-level wind over the continental United States (lower), as diagnosed from the National Centers for Environmental Prediction (NCEP)–National Center for Atmospheric Research (NCAR) reanalysis (Kalnay et al. 1996). The seasonal cycle of tornado counts and the southerly low-level meridional wind field show a similar evolution throughout the spring, with each decaying thereafter, although tornado counts decay much more rapidly through the summer months (upper). The AMJ climatological Great Plains low-level jet (GPLLJ) is clearly evident by the wind maxima over central Texas thrusting northward into the upper Midwest (lower). While weaker, the mean 850-hPa southerly flow extends eastward to the southeast coast of the United States encompassing much of the eastern two-thirds of the United States.

The data sources and methodology will be described in section 2. NALLJ variability and its regional impact on tornadic activity will be discussed in section 3. Section 4 documents the regional impact of NALLJ's on thermodynamic parameters conducive to tornado activity. Section 5 will assess the large-scale climate context, diagnosed through the connectivity of NALLJ's and U.S. tornadic activity to global SST variability, while section 6 is left for the concluding remarks.

2. Data and methodology

The SPC severe weather database is used to extract monthly tornado counts over the continental United States and a subset of regions (defined in section 3) for the years 1950–2010. Seasonal tornado indices are formed by subtracting the AMJ long-term 1950–2010 climatology from each year's AMJ season to obtain the corresponding tornado count anomaly. Given the potential for double counting of an individual tornado we only use the report that coincides with a tornado touchdown. Since there is some indication that weaker tornado counts may be unduly influenced by reporting inconsistencies over the period of record, two different thresholds are used in various subsequent analysis sections to create the seasonal tornado indices. The two indices are based on all tornado counts F0–F5 and F2–F5 tornado counts only. Furthermore, the F0–F5 reports were subject to a linear detrending to ameliorate the effects of changes in population, tornado assessment practices, National Weather Service guidelines, and other inhomogeneities. The bulk of the analysis uses the F0–F5 tornado indices and reflects our desire to cast a wide net with regard to seasonal severe weather and its relationship to NALLJ variability. Nevertheless, index choice sensitivity and comparisons are provided in the context of global SST variability to further the discussion regarding similarities and differences in using varying thresholds of tornadic indices derived from an imperfect damage-scale database. These characteristics are discussed more thoroughly in Brooks et al. (2003) and Doswell et al. (2009).

NALLJ variability for the 1950–2010 period is assessed by conducting an empirical orthogonal function (EOF) analysis on the seasonal anomalies of AMJ 850-hPa meridional wind field over the domain 105°–80°W, 20°–50°N in the NCEP–NCAR reanalysis. As in Weaver and Nigam (2008) a covariance-based analysis on the latitudinally weighted field was performed. The EOFs are not rotated given the limited analysis domain. The principal components obtained from this analysis are used as indices in relating NALLJ variability to AMJ seasonal tornadic activity, the thermodynamic environment, and global SST variations through correlation and regression analysis. While more modern reanalyses are available from various operational and research centers, none possess a historical record long enough as the NCEP–NCAR reanalysis to temporally align with the SPC tornado database.

To investigate the thermodynamic environment important for tornadic activity we apply NALLJ principal component (PC) regressions to select parameters from the brand new state-of-the-art Climate Forecast System Reanalysis (CFSR) (Saha et al. 2010). This new reanalysis system takes advantage of significant modeling and data assimilation upgrades developed in the ~15 years since the generation of the NCEP–NCAR reanalysis. As such we use it here to assess anomalies of mixed layer convective available potential energy (CAPE), 1000–500-hPa wind shear (SHEAR), and 0–3000-m storm relative helicity (HLCY), which are all important indicators of potential tornadic activity. Despite the truncated (1979–2010) record in the CFSR as compared to the NCEP–NCAR reanalysis, the dependence of these thermodynamic parameters on features of the assimilating model necessitates that we use the latest technological advances in reanalysis for assessing these linkages.

SST and precipitation linkages are similarly ascertained via correlation and regression analysis and are facilitated by using the Extended Reconstructed Sea Surface Temperature version 3 (ERSSTv3) (Smith et al. 2008) and precipitation reconstruction (PREC) (Chen et al. 2002).

3. Regional NALLJ and tornadoes

a. NALLJ modes

Shown in Fig. 2 are the first three EOF modes of NALLJ variability for the 1950–2010 (left), 1950–78 (middle), and 1979–2010 (right) analysis periods. The structure of NALLJ variability modes are derived from the AMJ PC regressions to 850-hPa meridional wind (contoured) over the 1950–2010, 1950–78, and

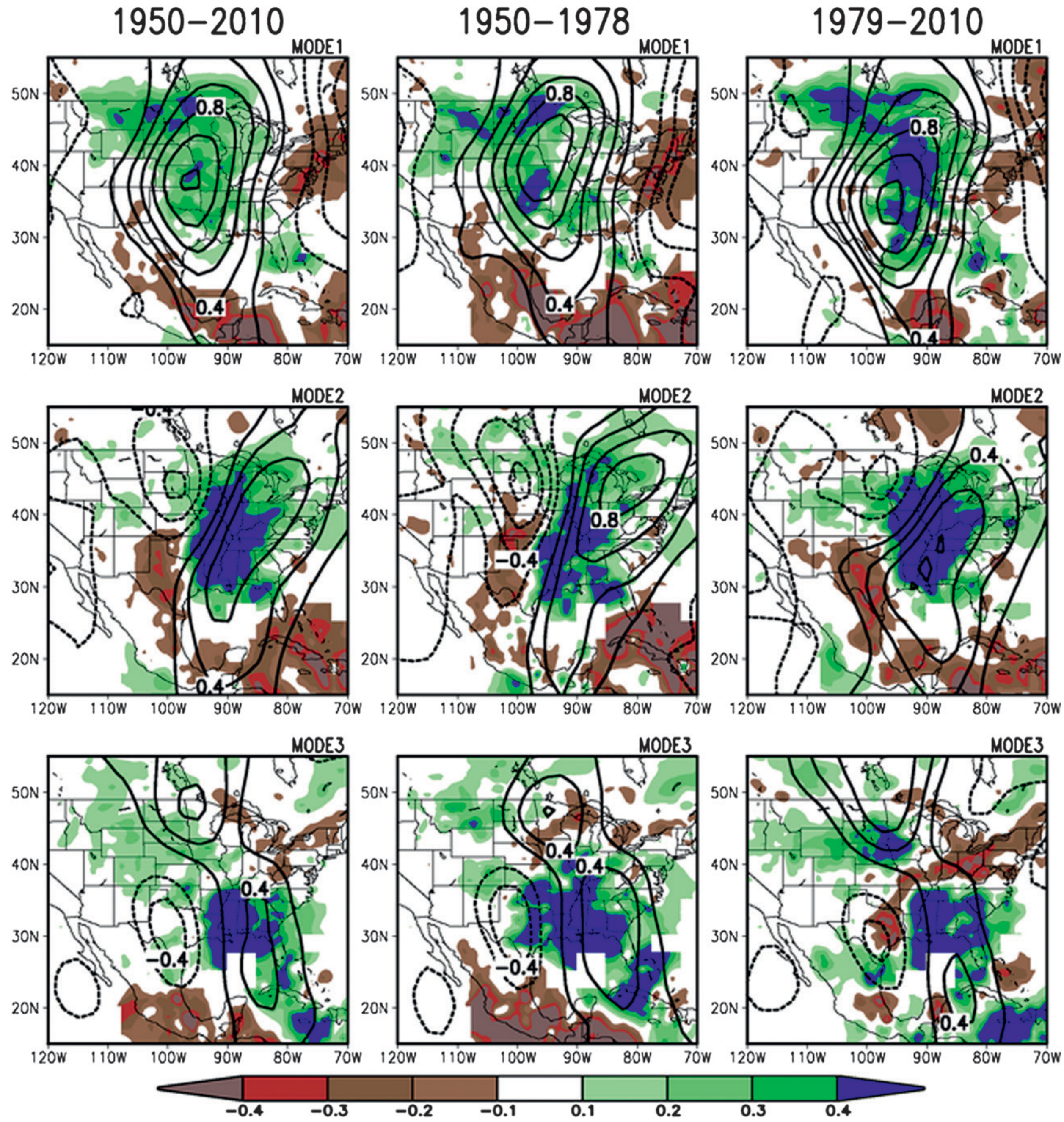

FIG. 2. Recurrent patterns of AMJ NALLJ variability (contours) and regressed precipitation (shaded) for (left) 1950–2010, (middle) 1950–78, and (right) 1979–2010. The EOF modes are contoured at 0.2 m s^{-1} and precipitation is shaded at 0.1 mm day^{-1}.

1979–2010 time periods respectively. Similarly, the precipitation footprints (shaded) are diagnosed via PC time series regression to AMJ precipitation anomalies. Together the first three modes explain ~72% of the regional 850-hPa meridional wind variance with mode 1, mode 2, and mode 3 explaining 41%, 20%, and 11% of the variance, respectively.

NALLJ mode 1 is characterized by significant strengthening and expansion of the climatological GPLLJ, which is typically active in a narrow band between 95°–100°W and 25°–35°N (Fig. 1). This mode shows a widely distributed precipitation impact with areas of strong precipitation anomalies spread throughout the central and northern Great Plains, apparently a reflection of the enhanced moisture transport from the Gulf of Mexico.[1] While period changes may appear subtle upon first glance, it is noteworthy that mode 1 850-hPa wind and precipitation maxima are stronger and shifted southward during the 1979–2010 period as compared to 1950–78. The increased precipitation impact in the recent period is likely a manifestation of the stronger and deeper fetch to the tropical moisture source over the western Caribbean Sea and the Gulf of Mexico.

NALLJ mode 2 shows an anomalous jet structure characterized by opposing 850-hPa meridional wind anomalies converging over portions of the Great Plains and upper Midwest. As in mode 1 there is a deep penetration of tropical moisture, in this case into the southeastern U.S. Gulf States and Mississippi River basin. Similar to mode 1 the 850-hPa wind structure has shifted south with a larger maxima in precipitation when comparing the early and late periods. While the southerly anomalous flow is weaker in mode 2 as compared to mode 1 the precipitation and moisture flux convergence (MFC) (not shown) impact is actually more substantial on account of the enhanced convergence from the northerly low-level jet anomaly over the northern Plains.

Mode 3 is weaker than both modes 1 and 2, however, with comparable precipitation impacts over the Southeast. The meridional wind of mode 3 shows an anomalous jet structure with southerly anomalies over the Southeast and northern Plains, and a northerly anomaly over the southern Great Plains, essentially shifting the climatological low-level jet northward and/or eastward. Period differences are reflected by subtle wind structure shifts and an erosion of the southern precipitation maxima on its western edge during the latter period, most notably over Texas.

b. *Regional tornado and NALLJ variability*

The NALLJ patterns (cf. Fig. 2) point to three key regions for further analysis, the northern Great Plains (NGP), southern Great Plains (SGP), and Southeast (SE). While the anomalous meridional wind and precipitation patterns do not explicitly identify clearly separable latitude and longitude boundaries (i.e., some overlap exists), the regional precipitation (Fig. 2) and MFC (not shown) impacts provide sufficient guidance for choosing suitable tornado analysis regions, especially given the presence of significant moisture and dynamic convergence promoted by low-level jet development, which are essential ingredients to the severe storm environment.

[1] This mode has a much more focused NGP precipitation footprint during mid–late summer [i.e., July–September (JAS)] and was a major instigator of the July 1993 Midwest floods (Weaver and Nigam 2011).

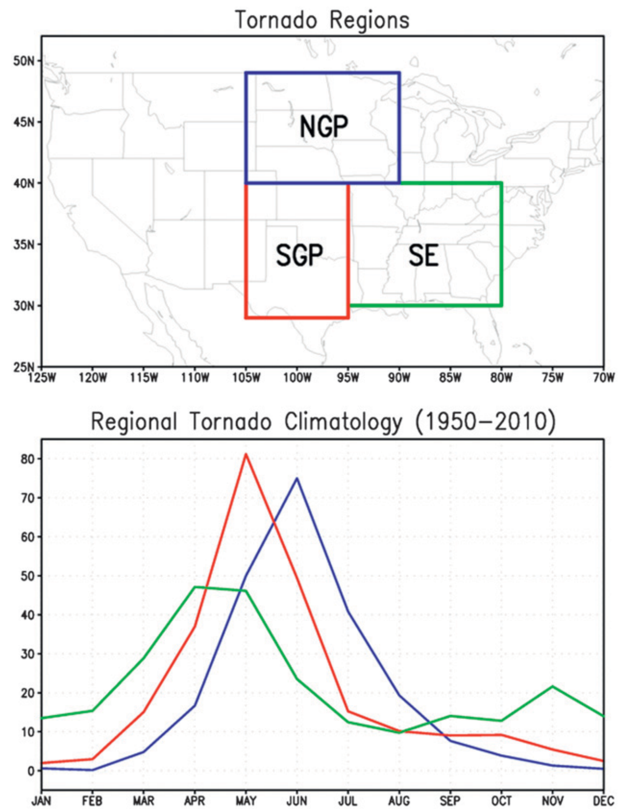

FIG. 3. (top) Areas defining the three regional tornado indices: SGP, NGP, and SE. (bottom) Monthly climatology of tornado counts corresponding to the three tornado regions. SGP, NGP, and SE are denoted by the red, blue, and green lines, respectively.

As such, Fig. 3 (upper) identifies the three tornado analysis regions and the 1950–2010 monthly climatology of tornado counts (lower) for the respective regions. The regions are the NGP 40°–49°N, 95°–105°W (blue); SGP 29°–40°N, 95°–105°W (red); and SE 30°–40°N, 80°–90°W (green). The NGP and SGP regions have sharply defined climatological peaks and are the strongest (not surprising given the collocation with "Tornado Alley"); however, the SGP reaches its maximum in May, while in the NGP the climatological peak tornadic activity is in June. The Southeast exhibits a double peak during April and May, placing the AMJ total on par with both the NGP and SGP.

Figure 4 shows the three regional detrended tornado indices: NGP (blue bar), SE (green bar), and SGP (red bar). Even in detrended tornado data there appear persistent negative anomalies throughout the early parts of the record (1950–79) for all three regions, except for 1957, 1965, 1973/74, and 1982. However, since about 1980 there has been increasing interannual variability, and with the exception of the latter half of the 1980s a preference for positive tornado anomalies and increased intraregional variability (i.e., regions with

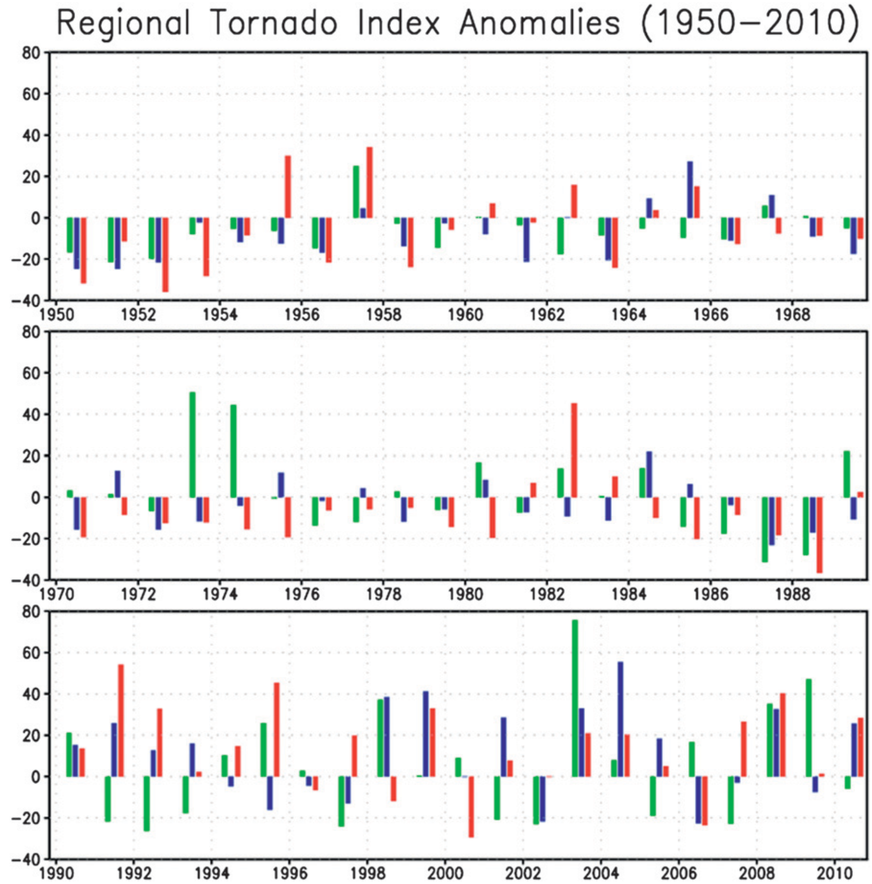

FIG. 4. Detrended AMJ tornado index anomalies for the SE (green), NGP (blue), and SGP (red) for 1950–2010.

opposite signed anomalies in the same year).[2] Some historically significant tornado seasons are evident, including 1973/74, and 2003, which are dominated by SE tornado counts, and 1991 and 2008, which were more evenly distributed among the three regions. Persistent negative tornado anomalies are also present during the early 1950s and late 1980s.

Figure 5 shows the PC time series of regional NALLJ activity. Mode 1 (upper) exhibits interannual and decadal variability, with the decadal variability evident by the mostly positive values of this PC during the early years of the period (1950–78) and more negative values in the latter 1979–2010 period. The PC time series for mode 2 (middle) shows much stronger interannual variation with no visually discernible decadal component, although there are same-sign groupings ranging from 2 to 10 consecutive years. Mode 3 (lower) exhibits much stronger interannual variability as compared to modes 1 and 2.

From visual inspection it appears that the NALLJ modes and the regional tornado indices may exhibit some degree of temporal association. This makes physical sense given that there is a regional preference for the three NALLJ modes as identified in their precipitation impact. Table 1 displays the temporal correlation coefficients between the three NALLJ PCs and the three tornado regions (cf. Fig. 3) for the 1950–2010, 1950–78, and 1979–2010 periods, with correlations highlighted in bold denoting the 95% statistical significance based on a t test. The correlations show interesting features, most notably the weaker (stronger) correlation of NALLJ PC 1 with the NGP (SGP) tornado indices during the 1950–78 (1979–2010). In fact the correlation between NALLJ PC 1 and the SGP has nearly doubled in the recent period, consistent with other recently discovered southward shifts in warm season regional climate variability mechanisms over the United States (Wang et al. 2010; Li

[2] These features may be dependent on the choice of strength threshold when creating the tornado index. Index sensitivity is discussed in section 5b.

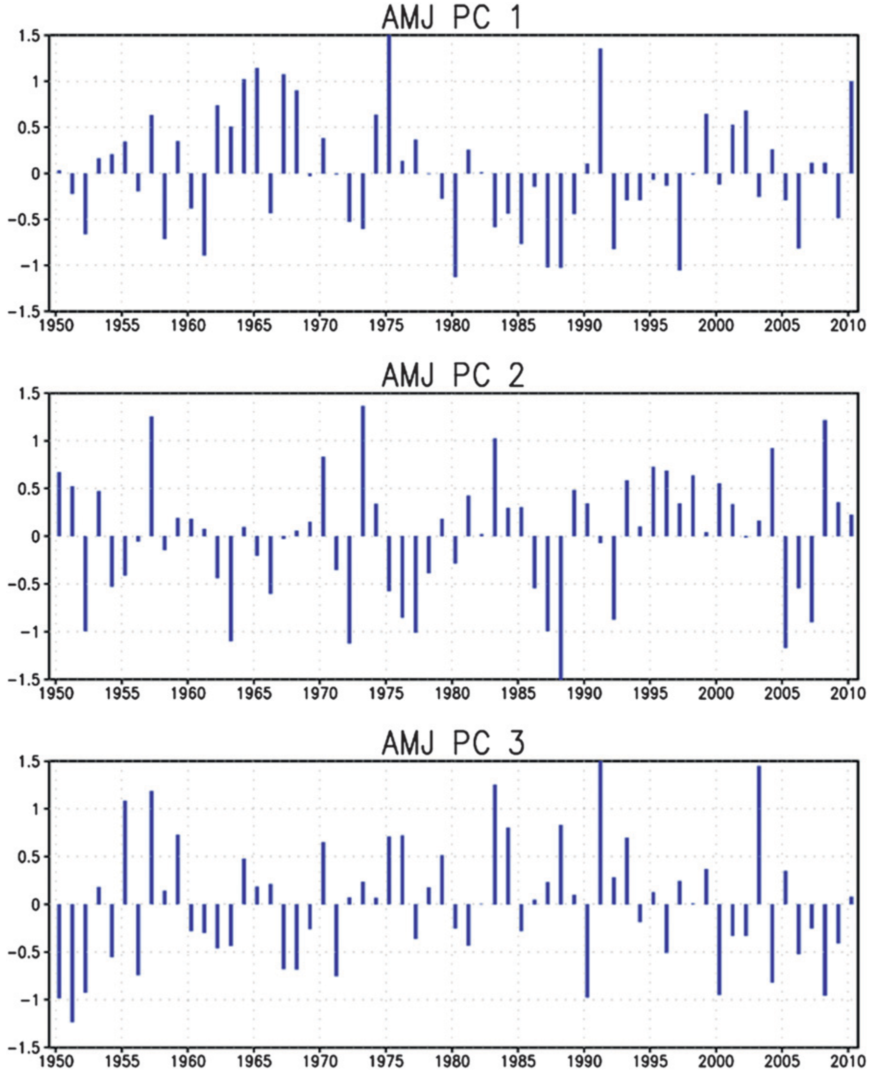

FIG. 5. AMJ PC index anomalies (m s^{-1}) for NALLJ (top) mode 1, (middle) mode 2, and (bottom) mode 3 for 1950–2010.

et al. 2011). NALLJ PC 2 has some degree of connectivity to all three regions in the 1979–2010 period; however, the connection to the SE is the only one that meets the significance test, although the increase in correlation coefficient over the early period is noteworthy. NALLJ PC 3 has significant correlations to all 3 regions, mostly during the early period; however, it has since exhibited very weak tornadic correlations.

4. Tornadic environment

The variations in NALLJ connectivity to regional tornadic activity bring to the forefront some intriguing questions, including the following. How does NALLJ mode 1 influence both the NGP and SGP especially during the more recent 1979–2010 period? Why and how does NALLJ mode 2 contribute to seasonal tornadic activity over all 3 regions in the recent period? Why is mode 3 so weakly correlated to all three tornado regions during 1979–2010, despite its strong precipitation impacts, deep tropical moisture fetch, and PC amplitude that is comparable to mode 2?[3]

To investigate these questions Fig. 6 shows NALLJ PC regressions to three environmental parameters that are traditionally linked to tornado activity (Djuric 1994). Seasonal AMJ anomalies of CAPE, 1000–500-hPa wind

[3] This implies that if PC 3 was used for reconstructions, the meridional wind and precipitation (or any other regressed parameter) amplitude would be comparable to mode 2, which has strong SE tornado correlations.

TABLE 1. Correlations of the regional tornado indices and the PC time series of NALLJ modes 1–3 for the periods 1950–2010, 1950–78, and 1979–2010. Correlations in boldface font denote those exceeding 95% significance based on a *t* test.

	PC 1	PC 2	PC 3
SE			
1950–2010	−0.02	**0.50**	0.05
1950–78	0.06	**0.53**	**0.32**
1979–2010	0.03	**0.47**	−0.15
NGP			
1950–2010	**0.35**	**0.24**	0.17
1950–78	**0.65**	0.05	**0.33**
1979–2010	**0.49**	0.28	0.03
SGP			
1950–2010	**0.30**	**0.24**	**0.29**
1950–78	**0.31**	0.13	**0.46**
1979–2010	**0.57**	0.25	0.13

shear (SHEAR), and HLCY from the CFSR were regressed against the three NALLJ PCs for 1979–2010. Positive anomalies of CAPE indicate enhanced atmospheric instability, while positive SHEAR and HLCY values indicate increased level of atmospheric shear, a necessary requirement for tornadic activity. Given that there is still considerable debate regarding the primacy of either SHEAR or HLCY in describing supercell dynamics (Weisman and Rotunno 2000), here both quantities are shown.

Mode 1 shows strong anomalies of CAPE from the Gulf Coast of Texas through the SGP and into the NGP with the largest CAPE values just to the east of the jet axis of this NALLJ mode (see Fig. 2). The maximum in SHEAR trisects all three tornado regions; however, it is strongest over the SGP and SE regions. The strongest HLCY is positioned to the west of the jet axis and has high values in both the southern and northern Great Plains, although favoring the NGP. It is noteworthy that despite high SHEAR and CAPE values over the SE the correlations between NALLJ PC 1 and the SE region are essentially zero, perhaps attesting to the importance of helicity in providing the favorable dynamic environment over the SGP and NGP regions, consistent with the stronger NALLJ PC 1 HLCY correlations there.

The structure for mode 2 exhibits substantial differences from those in mode 1. Although the CAPE maxima in the southeast corner of the NGP box is similar to that of mode 1, there is a sharp gradient of CAPE anomalies bisecting the northern and southern Great Plains on account of the eastward shift of the entire spatial pattern and the presence of the northerly anomalous NALLJ, which would inject drier and more stable air to the NGP, however, also strengthening the low-level convergence. Additionally, anomalous CAPE values associated with mode 2 are weaker in all regions as compared to mode 1 and especially the SE. The regressed shear is also weaker than in mode 1 with its maximum values occurring over the NGP. The HLCY pattern is much stronger in mode 2 than in either mode 1 or 3 and although the maxima is centered in the SGP box there are substantial anomalies throughout the SE region, not surprising given the rotational effects induced by meridional wind convergence at 850 hPa in this mode. While the strongest correlations between NALLJ PC 2 and the three tornado regions occur over the SE, recall that there is also some connectivity to the NGP and SGP, albeit weaker and potentially the result of stronger SHEAR (HLCY) over the NGP (SGP).

Recall that initially it was somewhat surprising that NALLJ mode 3 demonstrated such low correlations to all three tornado regions (Table 1), during the 1979–2010 period, given the strong moisture gradients over portions of each region. However, upon inspection of the tornadic parameters regressed against NALLJ PC 3 it is clear why this mode does not influence the tornadic environment in the recent period. Weak anomalies in all three fields are evident, and although there is a comparable amount of CAPE with respect to the mode 2 regressions, which can support warm season convective precipitation, there are negative SHEAR and HLCY anomalies, a situation that is detrimental to the tornadic environment.

5. Remote influences

SST anomalies, because of their slow evolution, have the potential to provide attribution and prediction capability on seasonal time scales. As such, it is important to assess the relationships of the NALLJ and tornado activity to the seasonal SST variability. Connectivity of U.S. tornadic activity to ENSO has proved inconclusive. While some of these studies did take into account the regionality of tornadoes and their linkage to traditional ENSO indices (Marzaban and Schaefer 2001; Daoust 2003; Muñoz and Enfield 2009), or provide a general description of regionality based on ENSO and annual tornado activity (Cook and Schaefer 2008), here we compare and contrast the spatial patterns of global SST variability during the early and latter periods of the record to the regional tornadic indices, and the NALLJ PCs 1 and 2 during AMJ, the peak of the tornado season.[4] This analysis strategy assumes no a priori assumption regarding the

[4] Given the unremarkable connection of NALLJ PC 3 to any of the three tornado regions in the recent period and the 11% percentage of explained variance we do not analyze the potential SST influence on this mode for brevity.

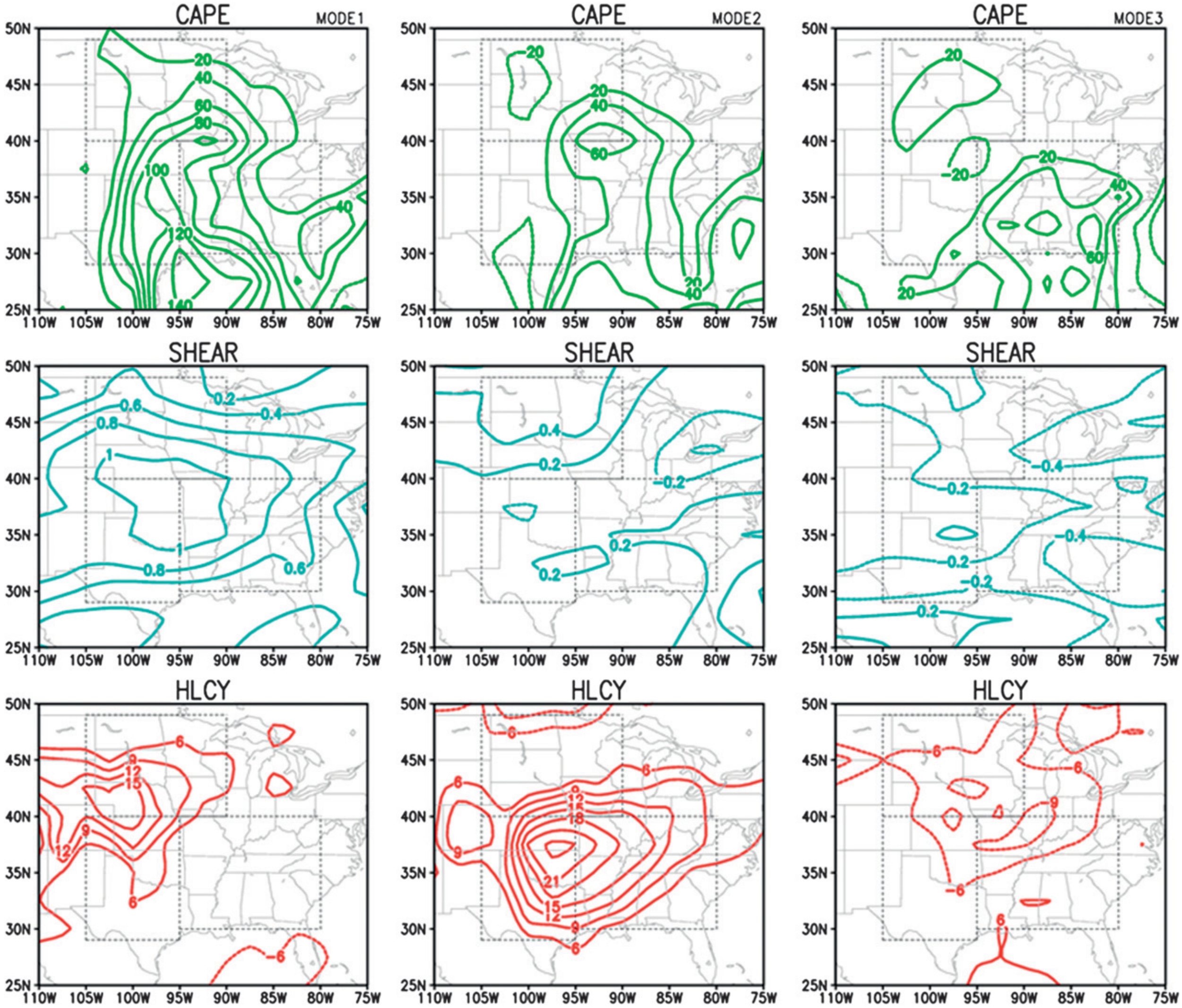

FIG. 6. NALLJ PC time series regressions to (top) CAPE, (middle) SHEAR, and (bottom) HLCY for (from left to right) mode 1, mode 2, and mode 3 for 1979–2010. CAPE is contoured at 20 J kg^{-1}, SHEAR at 0.2 m s^{-1}, and HLCY at 3 m^2 s^{-2}.

structure of the associated SST variability, as is the case when targeting connectivity to indices of ENSO variability.

a. Epochal sensitivity

The southward shift and intensification of the NALLJ modes and their related precipitation anomalies in the recent decades as compared to the earlier ones motivates an analysis of the characteristic SST patterns during these two epochs in conjunction with the full 61-yr SST record. Figures 7 and 8 show the NGP tornado (Fig. 7) and NALLJ PC 1 (Fig. 8) index correlations to SST variability over much of the global oceans for 1950–2010 (top), 1950–78 (middle), and 1979–2010 (lower). The NALLJ PC 1 and detrended NGP tornado indices show different correlation structures over the 1950–2010 period, with the NGP tornado index related to a global-scale SST warming pattern, while the NALLJ PC 1 shows connectivity to decadal variability structures in both the Atlantic and Pacific.

The origin of the discrepancy in the SST pattern correlation between the NGP tornado index and NALLJ PC 1 (Figs. 7 and 8, top panels) is intriguing. The NGP detrended index SST correlation structure bears a strong resemblance to the annual SST warming trend pattern in the observed twentieth-century record (see Fig. 1; Schubert et al. 2009). However, despite using a detrended tornado index it is unclear to the extent that this similarity to the twentieth-century SST trend is physically based since early record tornado reports are susceptible to artificial trends (Verbout et al. 2006; Doswell et al. 2009), and since no such SST pattern is

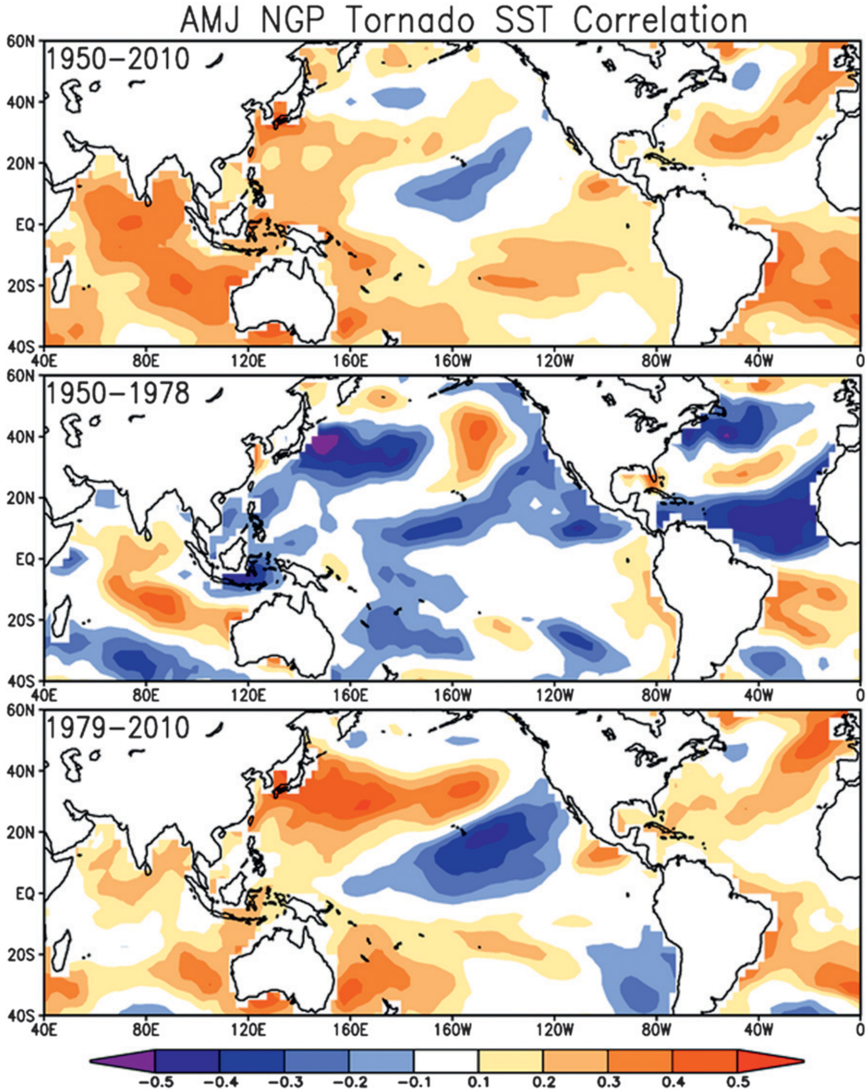

FIG. 7. AMJ NGP tornado index correlations to SST for (top) 1950–2010, (middle) 1950–78, and (bottom) 1979–2010. Correlations are shaded at 0.1 intervals.

detected in connection to NALLJ PC 1 (Fig. 8). Nevertheless, NALLJ variability is only one mechanism and likely not a singularly sufficient condition for seasonal tornadic activity, leaving open the possibility that there may be a physical connection outside of NALLJ variability between NGP tornadic activity and the observed SST warming trend.

The NALLJ PC 1 and tornado indices do show similar SST patterns when compared over the early and late time periods, respectively (Figs. 7 and 8, middle and bottom panels). Much of the epochal contrast in correlation emerges from the significant differences in the Atlantic basin where the early period bears a striking resemblance to the Atlantic multidecadal oscillation (AMO) SST pattern (Enfield et al. 2001; Guan and Nigam 2009). The latter period appears more like the PDO SST pattern (Mantua et al. 1997), including the warm tongue in the northeast Atlantic. (Although the PDO and AMO are basin centric, they have spatial correlation to other ocean basins. See http://www.esrl.noaa.gov/psd/data/correlation/ for AMJ AMO and PDO global SST and atmospheric circulation correlations.)

NALLJ mode 2 is most strongly connected to the tornadic activity in SE region, recalling the correlation between PC 2 and the SE tornado index (Table 1). Figures 9 and 10 show the SE tornado (Fig. 9) and NALLJ PC 2 (Fig. 10) index correlations to SST anomalies over much of the global oceans for 1950–2010 (top), 1950–78 (middle) and 1979–2010 (lower). The global SST correlations over the 1950–2010 period are

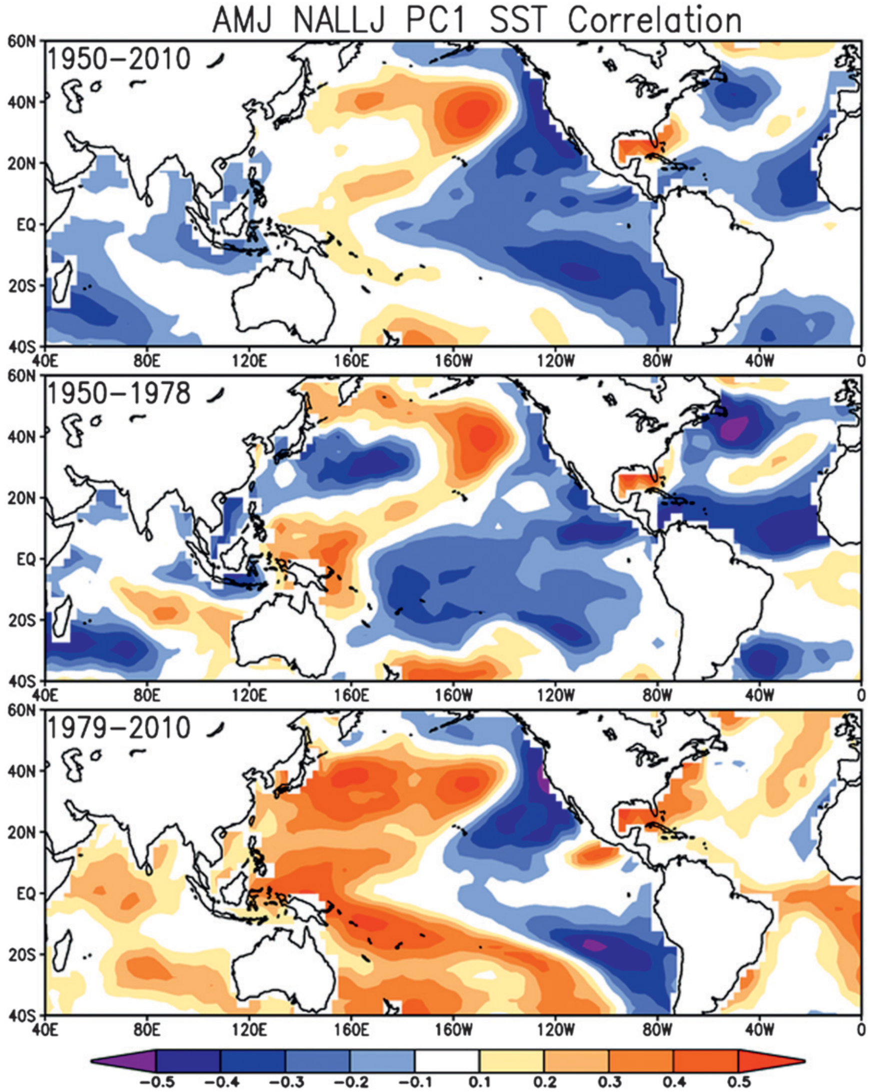

FIG. 8. AMJ NALLJ PC 1 correlations to SST for (top) 1950–2010, (middle) 1950–78, and (bottom) 1979–2010. Correlations are shaded at 0.1 intervals.

weak for both the SE tornado and NALLJ PC 2 indices and do not show a similar preference for the SST warming trend pattern. This is in stark contrast to the NGP in that there is no discernible connection of the F0–F5 SE tornado index to the SST trend pattern.

While the SE tornado index and NALLJ PC 2 exhibits almost no connectivity to the tropical Pacific during the 1950–78 period, especially over the ENSO region, the Atlantic shows much stronger correlations for the SE tornado index, again reminiscent of the AMO pattern. Although the NALLJ PC 2 correlations are generally weaker over the Atlantic, they do contain vestiges of the SE tornado correlation structure over the northern Atlantic, subtropical western Atlantic, and South Atlantic regions.

The latter period of 1979–2010 (lower) is devoid of the AMO-like correlation structure; however, it is highlighted by the central tropical Pacific connectivity, although still quite weak in the SE tornado index case. The tropical Pacific SST structure of the NALLJ PC 2 appears similar to the ENSO Modoki, a mode of SST variability characterized by larger amplitude over the tropical central Pacific Ocean when compared to the eastern portion of the tropical Pacific basin (Ashok et al. 2007). The appearance of a relative difference in SST between the east and central Pacific has recently been connected to total U.S tornado variability over the months of April and May via the Trans Niño Index (S.-K. Lee et al. 2012, unpublished manuscript). The SST structure here hints that the connection may be

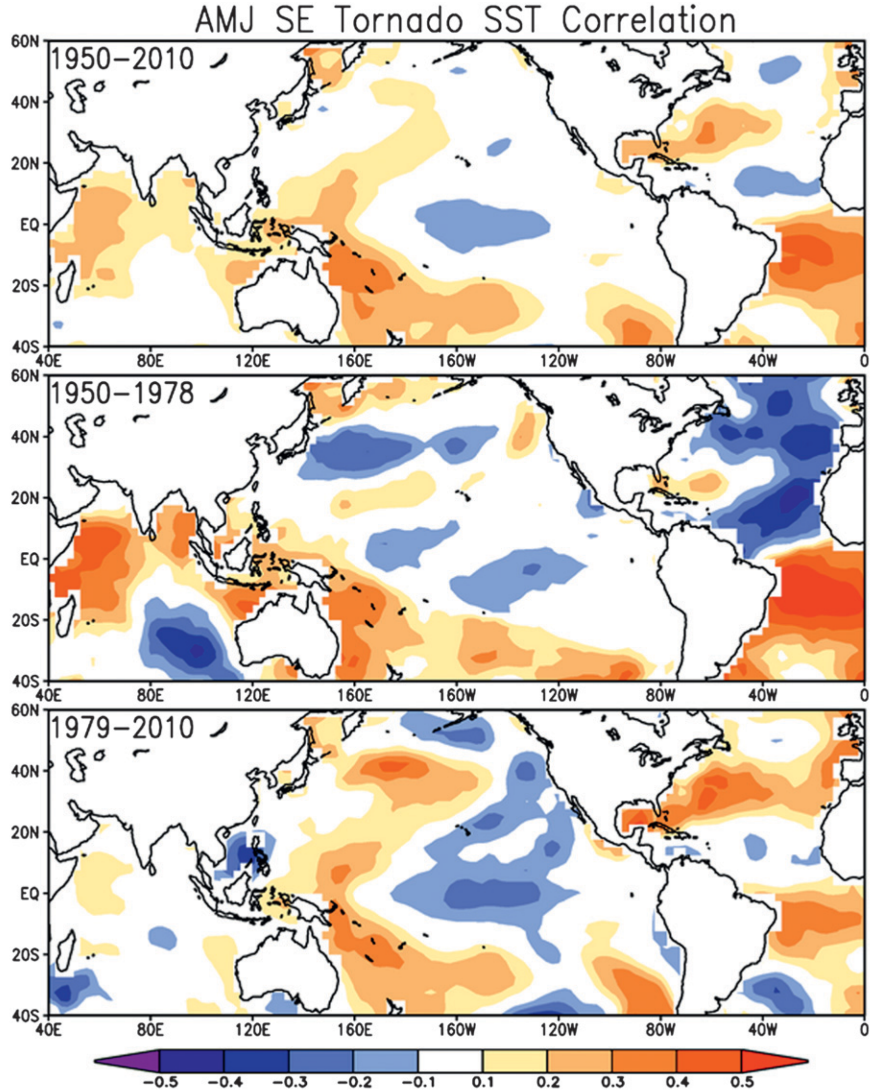

FIG. 9. SE tornado index correlations to SST for (top) 1950–2010, (middle) 1950–78, and (bottom) 1979–2010 for AMJ. Correlations are shaded at 0.1 intervals.

further clarified as one related to tornadic activity over the SE region of the United States.

It is reasonable to question how NALLJ variability is similarly influenced by SST variations in separate ocean basins. One of the complexities with regard to NALLJ variability is its susceptibility to various mechanisms of influence. NALLJ shifting and intensification may be related to spatial shifts in the upper-level zonal jet (Uccelini and Johnson 1979) and fluctuations in Atlantic basin mean sea level pressure (Weaver et al. 2009b). An assessment of the characteristic patterns of these fields related to the AMO and PDO reveals that during AMJ the cold phase of the PDO is likely to induce a southward shift of the upper level 200-hPa zonal jet over North America, while a cold AMO increases the mean sea level pressure gradient over the central United States (figures not shown). As it pertains to the early period Atlantic versus late period Pacific influences on NALLJ variability and by extension tornadic activity, this may partially explain the southward shift of the NALLJ's as one related to the similarly shifted upper level jet, consistent with the cold phase of the PDO.

b. *Tornado index sensitivity*

It has been documented that U.S. F0 tornado reports may be susceptible to artificial changes in reporting methodology (Verbout et al. 2006) and that limiting the analysis of historical tornado information to the stronger F2–F5 tornado counts may be more reliable (Doswell

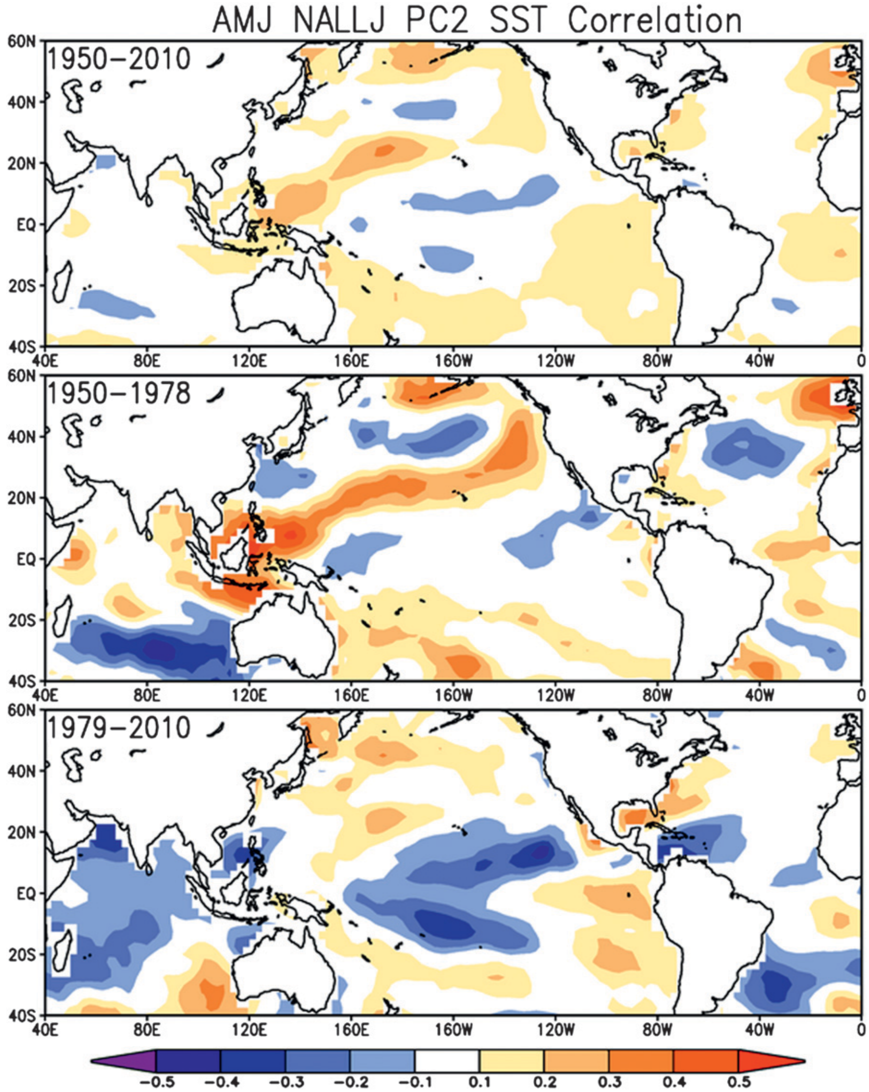

FIG. 10. AMJ NALLJ correlations to SST for (top) 1950–2010, (middle) 1950–78, and (bottom) 1979–2010. Correlations are shaded at 0.1 intervals.

et al. 2009). Despite using detrended tornado indices in this study, it is possible that including the full F0–F5 record may bias the SST correlation structure. Conversely, not including the weaker tornado reports may also bias the results since the climatic factors that produce strong tornadoes (e.g., F2+) may not occur as often or be identical to those of a weaker tornadic set up, potentially obscuring a more complete understanding of the seasonal severe weather environment. Nevertheless, Figs. 11 and 12 show the NGP and SE tornado index correlations to SST anomalies using only F2–F5 category tornado indices for 1950–2010 (top), 1950–78 (middle), and 1979–2010 (bottom).

The 1950–2010 F2–F5 NGP tornado index correlations (Fig. 11, top panel) show a global-scale SST cooling pattern. As in the NGP F0–F5 SST structure (Fig. 7), the pattern is similar to the twentieth-century SST trend structure of Schubert et al. (2009), although in the F2–F5 case it is opposite in sign. This indicates that the observed warming trend in SST over the last 61 years is related to a reduction in the number of F2 and greater tornadoes over the NGP region in favor of weaker F0–F1 tornadoes. The early and late periods similarly identify the Atlantic (early period) and Pacific (late period) connectivity as in the F0–F5 record.

The 1950–2010 F2–F5 SE tornado index correlations (top panel, Fig. 12) show a correlation structure that is similar to that from the F0–F5 tornado index, as seen in the cold and warm action centers over the central equatorial Pacific and Atlantic and the northern and southern

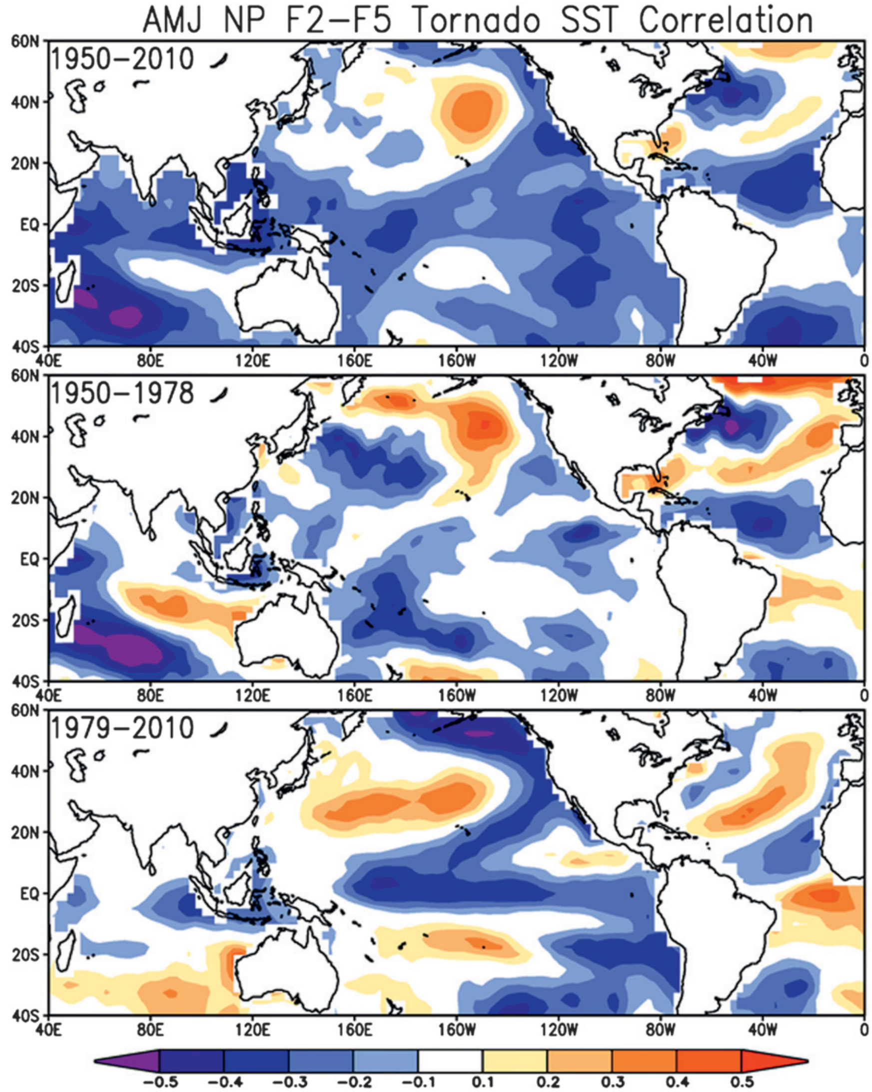

FIG. 11. AMJ NGP F2–F5 tornado index correlations to SST for (top) 1950–2010, (middle) 1950–78, and (bottom) 1979–2010. Correlations are shaded at 0.1 intervals.

midlatitude Atlantic Ocean (Fig. 9).[5] The early and recent periods appear dominated by Atlantic and Pacific SST variability modes respectively, just as in the SE F0–F5 case. The consistency of the SE tornado SST correlation structure amongst varying tornado index choices suggests that the SE has little connection to either the observed global SST trend or is being influenced by a spurious trend from inadequate reporting when compared to the NGP region. The origin of this discrepancy is important in the context of previous analyses, which typically describe the tornado reporting (and other) biases in a total U.S. framework. The results indicate that if the reporting biases are important in the climatic context of the current analysis strategy here, then the SE is immune to these biases, for reasons not known. An alternative explanation is the possibility that the NGP region has a greater climatic sensitivity to the trend pattern in SST.

To further explore this regional discrepancy Fig. 13 shows the F2–F5 tornado index anomalies for 1950–2010 plotted as in Fig. 4. At first glance the F2–F5 tornado indices share many of the same features as the F0–F5 indices; the negative anomalies during the 1950s, the strong outbreaks during 1973/74, and the late 1980s negative tornado anomalies. However, during 1990–2010 the

[5] Relaxing the correlation plotting threshold in Fig. 9 to 0.05 shows a nearly identical pattern to that in Fig. 12.

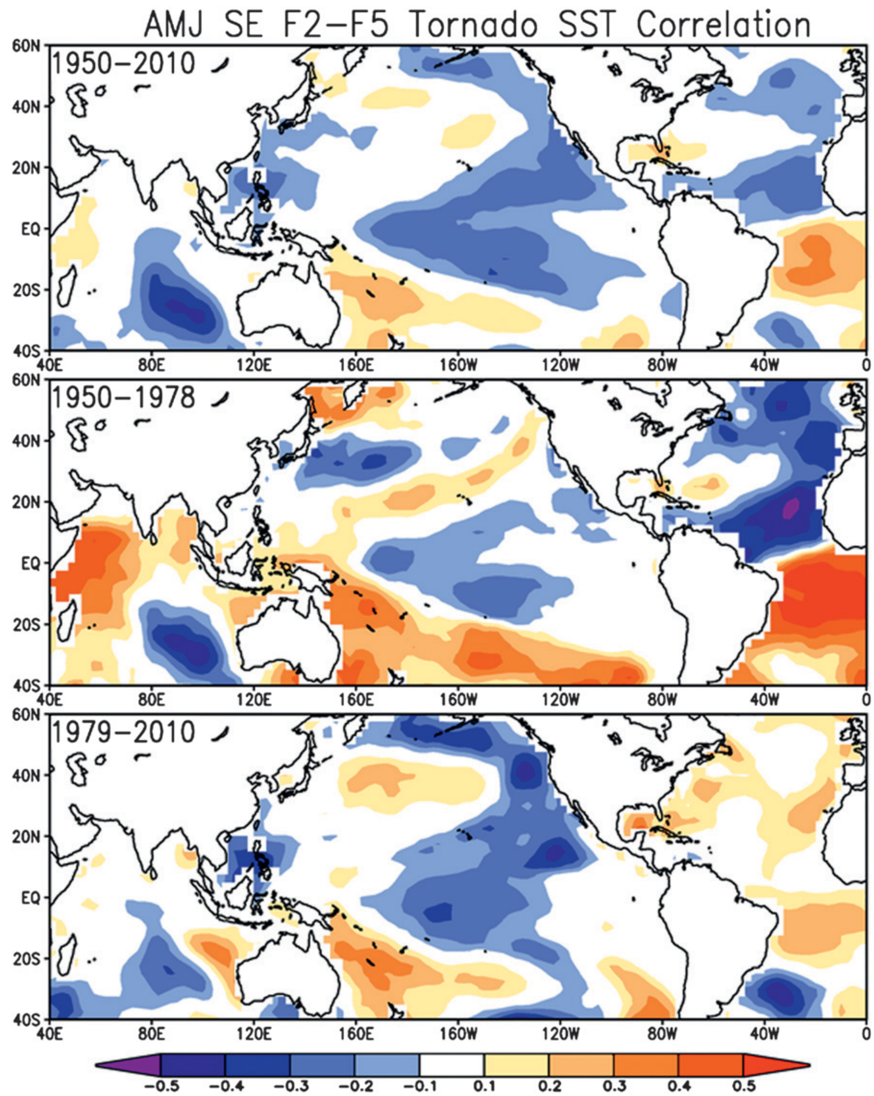

FIG. 12. AMJ SE F2–F5 tornado index correlations to SST for (top) 1950–2010, (middle) 1950–78, and (bottom) 1979–2010. Correlations are shaded at 0.1 intervals.

two indices diverge, with the F2–F5 index showing mostly negative anomalies in comparison with its detrended F0–F5 counterpart.

To more easily quantify the temporal association between the F0–F5 and F2–F5 indices Table 2 shows the correlation between these two tornado indices as a function of time period and region. As in the SST analysis, the F0–F5 and F2–F5 tornado indices over the SE (and SGP) region correlate well regardless of the chosen time period, further attesting to the immunity of the SE region to the apparent weaknesses in tornado reporting practices commonly referred to in many previous studies (Brooks et al. 2003; Verbout et al. 2006; Doswell et al. 2009). The NGP has the weakest correlation between the F0–F5 and F2–F5 indices, most notably during the recent 1979–2010 period, consistent with the SST trend contributing to an increase in F0–F1 tornadoes and a decrease in F2–F5 tornadoes over the NGP.

6. Concluding remarks

Variability of springtime tornadic activity over the United States is assessed from the perspective of regional tornado indices and distinct modes of NALLJ variability. The assessment is important for understanding the role that NALLJs have in seasonal tornadic activity as NALLJs are an extremely important driver of warm season climatic anomalies and extreme events over the United States. The selection of tornadic regions is facilitated by analyzing the seasonal precipitation

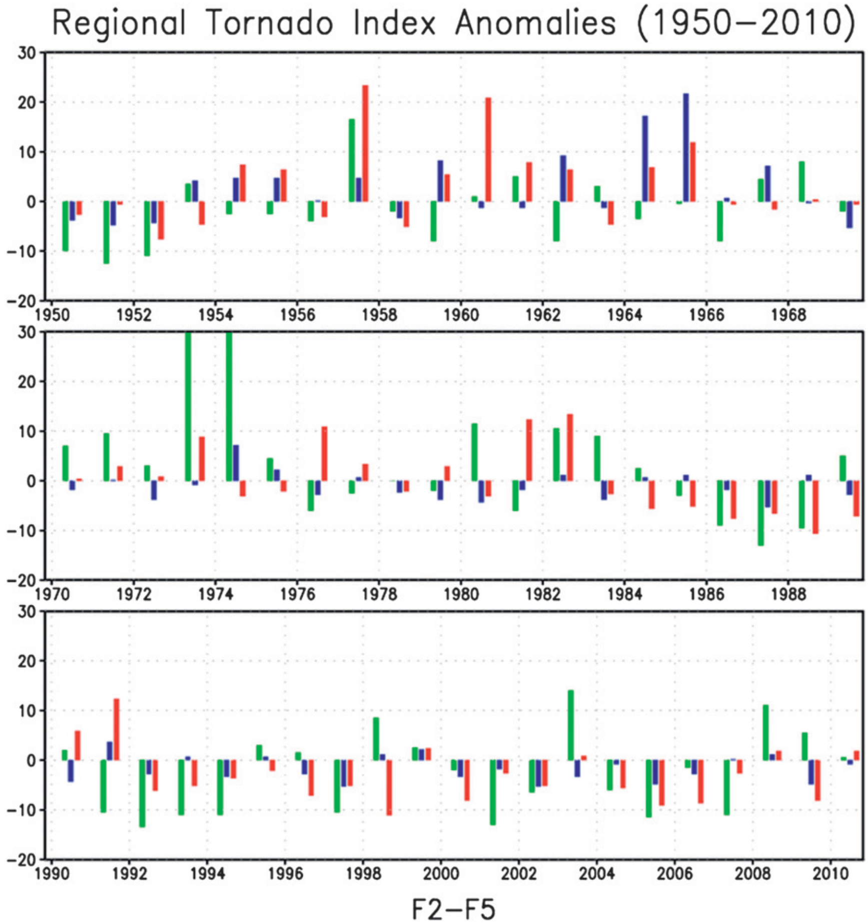

FIG. 13. AMJ F2–F5 tornado index anomalies for the SE (green), NGP (blue), and SGP (red) for 1950–2010.

impacts of the various NALLJ modes. Seasonal tornado and NALLJ activity is further framed in a large-scale climate context by assessing their connectivity to global SST variability. This is especially important given the inconclusiveness of recent studies regarding the linkage of tornadic activity to ENSO, and the potential inhomogeneities in the historical tornado database, a limitation not seen in the large-scale meridional wind field from consistent reanalysis systems.

It is found that preferred modes of NALLJ activity are linked to tornadic activity in three key regions: the Southeast and the northern and southern Great Plains. The NALLJ influence exhibits a multidecadal variation characterized by southward shifts of the jet core in all three NALLJ variability modes in the most recent decades as compared to the previous ones. This change is highlighted by the SGP tornado index nearly doubling its correlation with the NALLJ PC 1 in the recent 32-yr period. The influence of NALLJ on the tornadic environment is evidently through its impact on regional anomalies of CAPE, SHEAR, and HLCY. While all three NALLJ modes produce relatively similar CAPE anomalies they differ in their associated HLCY and SHEAR with modes 1 and 2 dominated by SHEAR and HLCY respectively, demonstrating the importance of both of these dynamic fields in analyzing the seasonal tornadic environment.

The remote SST variability linked to the NALLJ modes and regional tornado indices indicates a preference for the AMO (PDO) SST structure in the 1950–78 (1979–2010) period. Expanding the analysis period to

TABLE 2. Correlations of the regional F0–F5 and F2–F5 tornado indices for 1950–2010, 1950–78, and 1979–2010. All correlations exceed 95% significance based on a *t* test.

	SE	NGP	SGP
1950–2010	0.78	0.30	0.45
1950–78	0.95	0.75	0.79
1979–2010	0.82	0.43	0.62

the full 61-yr record reveals that the NGP tornado index is linked to an SST structure much like the observed SST trend pattern and more specifically a preference for a positive trend in the full range (F0–F5) of tornado strengths at the expense of the stronger F2+ activity. The discrepancy in the tornadic index strength sensitivity between the SE and NGP during AMJ is intriguing and to our knowledge has not been previously reported. While it is indisputable that tornado reporting has been influenced by factors outside of natural climate variability and change, it is not clear to what extent, if any, these potential inconsistencies have had with regard to the particular analysis strategy here and the results of this study. Were the reporting inconsistencies to have a significant impact it would be reasonable to expect that this effect would be distributed across all three regions, instead of just one, and in this case the NGP.

At a minimum it cannot be ruled out that the connection between the NGP tornadic activity and the recently observed SST warming trend is physically based, especially in light of recent analyses that support this notion. Diffenbaugh et al. (2008) discuss the likely influences of global warming on tornado activity. They conclude that global warming will impact the frequency, spatial distribution, and seasonal tornado activity through changes in CAPE and shear, characterized by an increase in CAPE through augmentation of temperature and humidity, and a decrease in shear through a weakened meridional temperature gradient. The result of these potential changes to CAPE and shear is that regions that experience peak tornado activity (i.e., F2+) may see reductions because of weakened shear; however, these reductions may be offset by increases in CAPE. The reduction in shear and increase in CAPE is dynamically consistent with a decreasing amount of strong (F2+) tornadoes in favor of an increase in weaker tornadoes (as in the NGP analysis here) since the supercell thunderstorms that typically spawn the most violent tornadoes (F2+) form in strong vertical wind shear environments, while tornadoes that form in diminished shear environments are weaker, despite the presence of strong CAPE. Ongoing research is predicated on clarifying the extent of climate variability and change in other physical mechanisms important for seasonal severe weather variability since the NALLJ modes are only one mechanism important for the maintenance of the seasonal tornadic environment.

Acknowledgments. The authors thank Drs. Wanqiu Wang and Zeng-Zhen Hu for reviewing an early version of the manuscript and the two anonymous reviewers who provided constructive comments. We also appreciate the editorial guidance of Dr. James Renwick.

REFERENCES

Ashok, K., and Coauthors, 2007: El Niño Modoki and its possible teleconnection. *J. Geophys. Res.,* **112,** C11007, doi:10.1029/2006JC003798.

Barlow, M., S. Nigam, and E. H. Berbery, 2001: ENSO, Pacific decadal variability, and U.S. summertime precipitation, drought, and stream flow. *J. Climate,* **14,** 2105–2128.

Bell, G. D., and M. Chelliah, 2006: Leading tropical modes associated with interannual and multidecadal fluctuations in North Atlantic hurricane activity. *J. Climate,* **19,** 590–612.

Brooks, H. E., J. W. Lee, and J. P. Craven, 2003: The spatial distribution of severe thunderstorm and tornado environments from global reanalysis data. *Atmos. Res.,* **67–68,** 73–94.

Chen, M. P., P. Xie, J. E. Janowiak, and P. A. Arkin, 2002: Global land precipitation: A 50-yr monthly analysis based on gauge observations. *J. Hydrometeor.,* **3,** 249–266.

Cook, A. R., and J. T. Schaefer, 2008: The relation of El Niño–Southern Oscillation (ENSO) to winter tornado outbreaks. *Mon. Wea. Rev.,* **136,** 3121–3137.

Daoust, M., 2003: An analysis of tornado days in Missouri for the period 1950–2002. *Phys. Geogr.,* **24,** 467–487.

Diffenbaugh, N. S., R. J. Trapp, and H. Brooks, 2008: Does global warming influence tornado activity? *Eos, Trans. Amer. Geophys. Union,* **89,** 53, doi:10.1029/2008EO530001.

Djuric, D., 1994: *Weather Analysis*. Prentice-Hall Inc., 304 pp.

Doswell, C. A., III, H. E. Brooks, and N. Dotzek, 2009: On the implementation of the Enhanced Fujita Scale in the USA. *Atmos. Res.,* **93,** 554–563.

Enfield, D. B., A. M. Mestas-Nuñez, and P. J. Trimble, 2001: The Atlantic multidecadal oscillation and its relation to rainfall and river flows in the continental U.S. *Geophys. Res. Lett.,* **28,** 2077–2080.

Frye, J. D., and T. L. Mote, 2010: Convection initiation along soil moisture boundaries in the southern Great Plains. *Mon. Wea. Rev.,* **138,** 1140–1151.

Galway, J. G., 1979: Relationship between precipitation and tornado activity. *Water Resour. Res.,* **15,** 961–964.

Guan, B., and S. Nigam, 2009: Analysis of Atlantic SST variability factoring interbasin links and the secular trend: Clarified structure of the Atlantic multidecadal oscillation. *J. Climate,* **22,** 4228–4240.

Hu, Z.-Z., and B. Huang, 2009: Interferential impact of ENSO and PDO on dry and wet conditions in the U.S. Great Plains. *J. Climate,* **22,** 6047–6065.

Kalnay, E., and Coauthors, 1996: The NCEP/NCAR 40-Year Reanalysis Project. *Bull. Amer. Meteor. Soc.,* **77,** 437–471.

Li, W., L. Li, R. Fu, Y. Deng, and H. Wang, 2011: Changes to the North Atlantic subtropical high and its role in the intensification of summer rainfall variability in the southeastern United States. *J. Climate,* **24,** 1499–1506.

Mantua, N. J., and Coauthors, 1997: A Pacific interdecadal climate oscillation with impacts on salmon production. *Bull. Amer. Meteor. Soc.,* **78,** 1069–1079.

Marzaban, C., and J. T. Schaefer, 2001: The correlation between U.S. tornadoes and Pacific sea surface temperatures. *Mon. Wea. Rev.,* **129,** 884–895.

Muñoz, E., and D. Enfield, 2009: The boreal spring variability of the intra-Americas low-level jet and its relation with precipitation and tornadoes in the eastern United States. *Climate Dyn.,* **36,** 247–259, doi:10.1007/s00382-009-0688-3.

Saha, S., and Coauthors, 2010: The NCEP Climate Forecast System Reanalysis. *Bull. Amer. Meteor. Soc.,* **91,** 1015–1057.

Schaefer, J. T., and R. Edwards, 1999: The SPC tornado/severe thunderstorm database. Preprints, *11th Conf. on Applied Climatology,* Dallas, TX, Amer. Meteor. Soc., 215–220.

Schubert, S., and Coauthors, 2009: A U.S. CLIVAR project to assess and compare the responses of global climate models to drought-related SST forcing patterns: Overview and results. *J. Climate,* **22,** 5251–5272.

Shepherd, M., D. Niyogi, and T. L. Mote, 2009: A seasonal-scale climatological analysis correlating spring tornadic activity with antecedent fall-winter drought in the southeastern United States. *Environ. Res. Lett.,* **4,** 1–7.

Smith, T. M., R. W. Reynolds, T. C. Peterson, and J. Lawrimore, 2008: Improvements to NOAA's historical merged land–ocean surface temperature analysis. *J. Climate,* **21,** 2283–2296.

Tippett, M. K., A. H. Sobel, and S. J. Camargo, 2012: Association of U.S. tornado occurrence with monthly environmental parameters. *Geophys. Res. Lett,* **39,** L02801, doi:10.1029/2011GL050368.

Uccelini, L. W., and D. R. Johnson, 1979: The coupling of upper- and lower-tropospheric jet streaks and implications for the development of severe convective storms. *Mon. Wea. Rev.,* **107,** 682–703.

Verbout, S. M., H. E. Brooks, L. M. Leslie, and D. M. Schultz, 2006: Evolution of the U.S. tornado database: 1954–2003. *Wea. Forecasting,* **21,** 86–93.

Wang, H., and Coauthors, 2010: Intensification of summer rainfall variability in the southeastern United States during recent decades. *J. Hydrometeor.,* **11,** 1007–1018.

Weaver, S. J., and S. Nigam, 2008: Variability of the Great Plains low-level jet: Large-scale circulation context and hydroclimate impacts. *J. Climate,* **21,** 1532–1551.

——, and ——, 2011: Recurrent supersynoptic evolution of the Great Plains low-level jet. *J. Climate,* **24,** 575–582.

——, A. Ruiz-Barradas, and S. Nigam, 2009a: Pentad evolution of the 1988 drought and 1993 flood over the Great Plains: A NARR perspective on the atmospheric and terrestrial water balance. *J. Climate,* **22,** 5366–5384.

——, S. Schubert, and H. Wang, 2009b: Warm season variations in the low-level circulation and precipitation over the central United States in observations, AMIP simulations, and idealized SST experiments. *J. Climate,* **22,** 5401–5420.

Weisman, M. L., and R. Rotunno, 2000: The use of vertical wind shear versus helicity in interpreting supercell dynamics. *J. Atmos. Sci.,* **57,** 1452–1472.